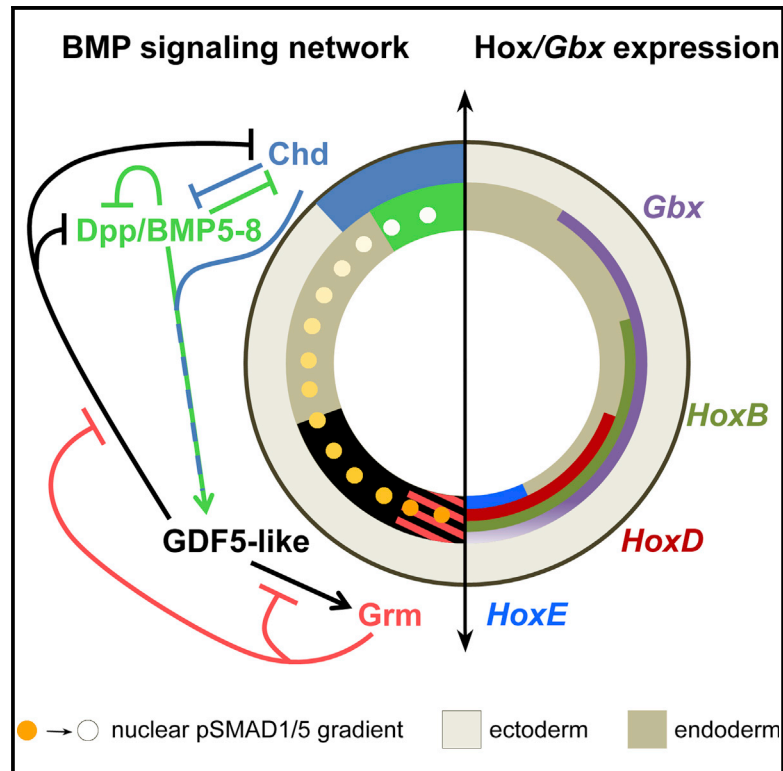


Axis Patterning by BMPs: Cnidarian Network Reveals Evolutionary Constraints

Graphical Abstract



Authors

Grigory Genikhovich, Patrick Fried, ...,
Dagmar Iber, Ulrich Technau

Correspondence

ulrich.technau@univie.ac.at

In Brief

Similar to Bilateria, anthozoans possess a secondary directive body axis. Genikhovich et al. examine the bone morphogenetic protein (BMP) signaling network required to compartmentalize the directive axis and regulate staggered Hox gene expression in a sea anemone. Mathematical modeling reveals the constraints guiding the evolution of the axis-forming BMP networks in animals.

Highlights

- A gradient of BMP signaling maintains the directive axis in *Nematostella*
- BMP signaling regulates *Nematostella* Hox genes and patterns the endoderm
- BMP network topology is similar in *Nematostella* and *Xenopus*
- Constraint analysis reveals the evolvability of BMP network components

Accession Numbers

KJ948110



Axis Patterning by BMPs: Cnidarian Network Reveals Evolutionary Constraints

Grigory Genikhovich,¹ Patrick Fried,^{2,3} M. Mandela Prünster,¹ Johannes B. Schinko,^{1,5} Anna F. Gilles,^{1,5} David Fredman,^{1,4} Karin Meier,² Dagmar Iber,^{2,3} and Ulrich Technau^{1,*}

¹Department for Molecular Evolution and Development, Centre of Organismal Systems Biology, University of Vienna, Althanstraße 14, 1090 Vienna, Austria

²Department for Biosystems Science and Engineering, ETH Zurich, Mattenstrasse 26, 4058 Basel, Switzerland

³Swiss Institute of Bioinformatics, Mattenstrasse 26, 4058 Basel, Switzerland

⁴Computational Biology Unit, University of Bergen, Thormøhlensgt. 55, 5008 Bergen, Norway

⁵Present address: Comparative Developmental Biology and Regeneration, Institut de Génétique Fonctionnelle de Lyon (IGFL), 32-34 Avenue Tony Garnier, Lyon 69007, France

*Correspondence: ulrich.technau@univie.ac.at

<http://dx.doi.org/10.1016/j.celrep.2015.02.035>

This is an open access article under the CC BY-NC-ND license (<http://creativecommons.org/licenses/by-nc-nd/3.0/>).

SUMMARY

BMP signaling plays a crucial role in the establishment of the dorso-ventral body axis in bilaterally symmetric animals. However, the topologies of the bone morphogenetic protein (BMP) signaling networks vary drastically in different animal groups, raising questions about the evolutionary constraints and evolvability of BMP signaling systems. Using loss-of-function analysis and mathematical modeling, we show that two signaling centers expressing different BMPs and BMP antagonists maintain the secondary axis of the sea anemone *Nematostella*. We demonstrate that BMP signaling is required for asymmetric *Hox* gene expression and mesentery formation. Computational analysis reveals that network parameters related to BMP4 and Chordin are constrained both in *Nematostella* and *Xenopus*, while those describing the BMP signaling modulators can vary significantly. Notably, only *chordin*, but not *bmp4* expression needs to be spatially restricted for robust signaling gradient formation. Our data provide an explanation of the evolvability of BMP signaling systems in axis formation throughout Eumetazoa.

INTRODUCTION

Bone morphogenetic protein (BMP) signaling regulates dorso-ventral (DV) axis patterning in Bilateria. Binding of a homo- or heterodimeric BMP ligand to the BMP receptor leads to phosphorylation of SMAD1/5/8, which enters the nucleus together with SMAD4 and regulates transcription of target genes (Plouhinec et al., 2011). Several BMP family molecules, BMP2/4, BMP5-8, ADMP, and Gdf5/6, use this pathway, however, the most prominent members of the family are BMP2/4 and BMP5-8. Signaling is regulated extracellularly by several antagonists, including Chordin, which binds to BMPs and prevents

them from binding their receptors (Piccolo et al., 1996). In contrast to other BMP antagonists, Chordin can be cleaved by Toll-oid metalloprotease, resulting in the release of active BMP ligand (Piccolo et al., 1997). Thus, Chordin acts as a BMP shuttle diffusing away from Chordin source and promoting signaling at a distance (Plouhinec et al., 2011).

These interactions form a BMP signaling gradient patterning the DV axis in vertebrates and insects, leading to the idea of a common evolutionary origin of the DV axis in Bilateria (Arendt and Nübler-Jung, 1994; De Robertis, 2008). Indeed, in vertebrates and in *Drosophila*, *bmp4* and *chordin* homologs are expressed at the opposite ends of the DV axis (Figure 1A), and the position of the CNS is defined by suppression of BMP signaling, independent of whether the CNS is dorsal, as in vertebrates, or ventral, as in flies. Yet, even within Bilateria, variations regarding expression domains and network topology exist. For example, sea urchin *bmp4* and *chordin* are co-expressed on the same side of the DV axis (Figure 1A; Lapraz et al., 2009), and many molecules were shown to play crucial roles in DV patterning in some phyla but not in others (Inomata et al., 2008, 2013; Jaźwińska et al., 1999; Lee et al., 2006; Reversade and De Robertis, 2005), which raises the question of the ancestral condition in Bilateria. In this respect Cnidaria, the sister group to Bilateria (Hejnal et al., 2009; Philippe et al., 2011), is pivotal for understanding the evolution of key bilaterian traits. Among cnidarians, Anthozoa (corals, sea anemones) encompass bilaterally symmetric animals with a directive axis orthogonal to the oral-aboral axis. Previous work demonstrated that the directive axis of the sea anemone *Nematostella vectensis* is marked by asymmetric expression of BMPs and BMP antagonists (Finnerty et al., 2004; Matus et al., 2006a, 2006b; Rentzsch et al., 2006; Saina et al., 2009), pointing at the possible common evolutionary origin of the directive axis and the bilaterian DV axis.

Surprisingly, expression domains of the *Nematostella* homologs of vertebrate *bmp4* and *chordin*, *NvDpp* and *NvChd*, are not opposed as in vertebrates and insects but become co-localized during gastrulation at the same side of the embryo (Rentzsch et al., 2006), as in sea urchin (Lapraz et al., 2009; Figures 1A and 1B). This symmetry break depends on BMP

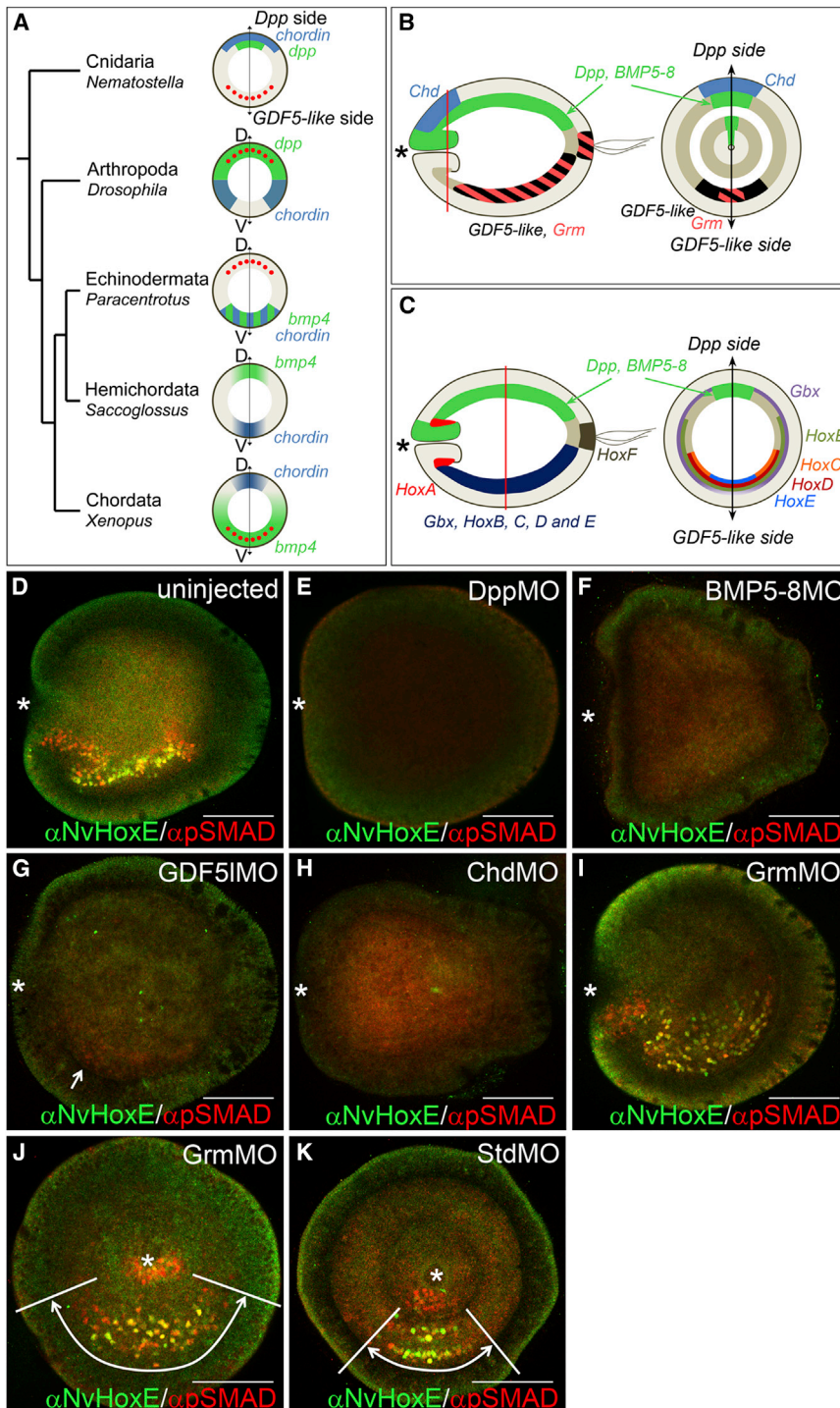


Figure 1. BMP Signaling Is Strongest on GDF5-like-Expressing Side of *Nematostella* Embryo

(A) Positions of *chordin* (blue) expression, *bmp4* (green) expression, and BMP signaling domain (red circles) in different animal models.

(B and C) Schematic representation of *NvDpp*, *NvBMP5-8*, *NvGDF5-like*, *NvChd*, *NvGrm*, *NvGbx*, and *Hox* expression domains in planula viewed laterally and orally. Red lines, cutting planes; black double-headed arrows, directive axis; asterisks, blastopore.

(D–K) The α pSMAD1/5 and α NvHoxE antibody staining in control and morphant early planulae, $n > 50$ for each sample; (D–I) lateral views; (J and K) oral views; asterisks, blastopore. (D) α pSMAD1/5-positive nuclei are located on NvHoxE-expressing side. α pSMAD1/5 and α NvHoxE stainings partially overlap. (E–K) α pSMAD1/5 and α NvHoxE in StdMO, ChdMO, GrmMO, GDF5IMO, BMP5-8MO, and DppMO embryos. Staining is absent in DppMO, BMP5-8MO, and ChdMO and suppressed (white arrow) in GDF5IMO (E–H); the domain showing strong staining (white double-headed arrows and white demarcating lines) is narrower in the StdMO than in the GrmMO (J and K).

See also Figure S1.

gene knockdown analysis and mathematical modeling, we reveal the functional links and constraints of the BMP signaling network regulating the maintenance of the directive axis in *Nematostella*. Our data provide an explanation for the evolutionary divergence of BMP-dependent axis regulation observed among animals.

RESULTS

BMP Signaling Forms a Gradient along the Directive Axis

Opposing expression of two sets of BMPs and BMP antagonists (*NvDpp*/*NvBMP5-8*/*NvChd* and *NvGDF5-like*/*NvGrm*) along the directive axis makes it difficult to predict how these secreted factors influence one another and where BMP signaling occurs. Using anti-pSMAD1/5 antibody staining as a readout of BMP signaling, we revealed strong nuclear pSMAD1/5 staining on

signaling itself (Saina et al., 2009). Another BMP gene, *NvGDF5-like*, and a gene coding for a BMP antagonist *gremlin* (*NvGrm*) also are expressed asymmetrically in early planula, yet on the opposite side of *NvDpp*, *NvBMP5-8*, and *NvChd* (Figure 1B), suggesting a more complex network (Rentzsch et al., 2006). How such signaling system evolved and what constraints limited its evolutionary divergence is unclear. Here, by a combination of

one side of the directive axis in early planula (Figure 1D). Since different BMPs are expressed on different sides of the embryo (Figure 1B; Table S1), and because no morphological landmarks exist, it was unclear where BMP signaling is active along the directive axis. Double in situ hybridization experiments showed that *NvDpp* and a *Hox* gene *NvHoxE* (Figures 1C and S1A; Table S2) are expressed on opposing sides of the directive axis

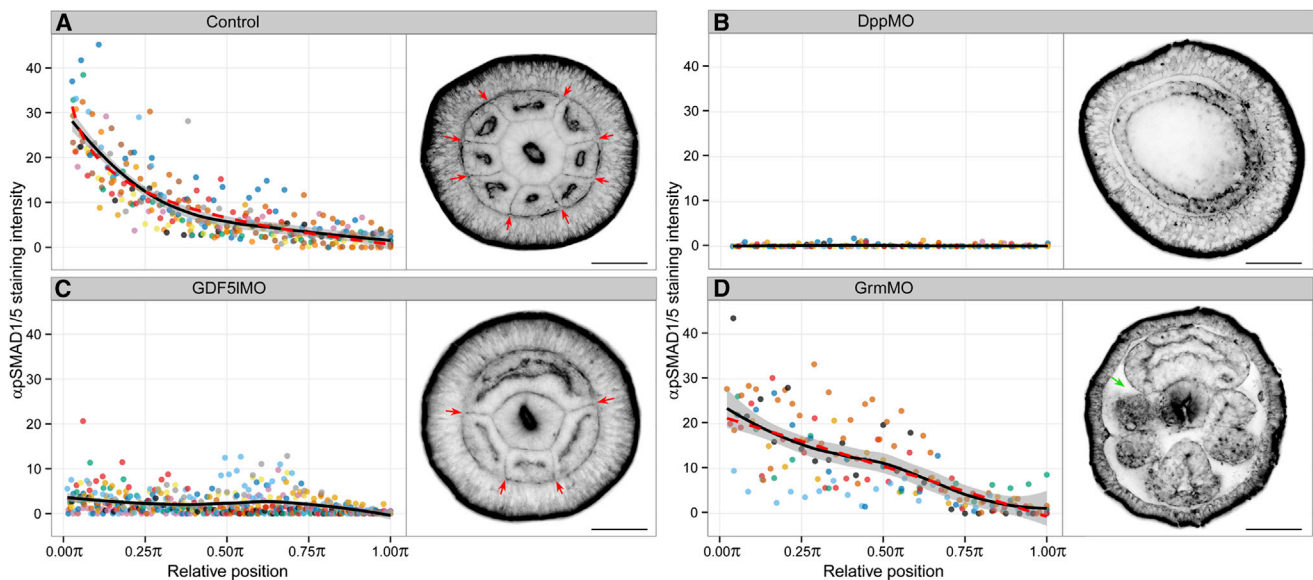


Figure 2. Effect of MO Knockdown on α pSMAD1/5 Staining Gradient and Morphology of Late Planulae

(A–D) Nuclear α pSMAD1/5 staining intensity as a function of relative position of each endodermal nucleus along 180° arc from 0 to π starting at the middle of pSMAD1/5-positive domain (see the [Supplemental Experimental Procedures](#) and [Figure S2A](#) for details on measuring), described by measurements from multiple embryos (colored points) for Control ($n = 12$), GrmMO ($n = 7$), GDF5IMO ($n = 10$), and DppMO ($n = 8$). LOESS smoothed curves (black lines) with 99% confidence interval for the mean (shade), and linear model fit of the logarithm of relative position to pSMAD1/5 staining intensity ($R^2 = 0.73$, dashed red line) for Control embryos and linear model fit of relative position to pSMAD1/5 staining intensity ($R^2 = 0.55$, dashed red line) for GrmMO embryos. Oral views of corresponding StdMO, DppMO, GDF5IMO, and GrmMO late planulae stained with fluorescent phalloidin are shown next to the graphs ($n > 55$ for each sample). While StdMO planulae with normal nuclear pSMAD1/5 gradient develop eight mesenteries (red arrows in A), DppMO-injected planulae lacking the pSMAD1/5 gradient do not develop mesenteries at all (B). α pSMAD1/5 staining intensity is suppressed but not absent in the GDF5IMO planulae correlating with the formation of four mesenteries instead of eight (red arrows in C). In GrmMO-treated embryos (D), the average pSMAD1/5 staining intensity is elevated in mid-range positions (see also [Figure S2C](#)) and more variable than in Control embryos across the whole range (see also [Figure S2D](#)). The endoderm in GrmMO appears compartmentalized but its development is abnormal with extremely thickened mesogloea (green arrow). Scale bars represent $50 \mu\text{m}$. See also [Figure S2](#).

([Finnerty et al., 2004](#); [Ryan et al., 2007](#)). Therefore, we generated an anti-NvHoxE antibody and co-immunostained the embryos with anti-pSMAD1/5 and anti-NvHoxE ([Figures 1C](#) and [S1](#)). We found that these two epitopes partially co-localized in the same endodermal nuclei on the *NvGDF5-like*-expressing side of the embryo, with additional pSMAD1/5 staining in the pharyngeal ectoderm ([Figures 1D](#) and [1K](#)). Thus, the peak of BMP signaling was found at a maximal distance to the source of NvDpp protein.

To assess the role of various BMPs and BMP antagonists in establishing pSMAD1/5 signaling, we performed antisense morpholino (MO)-mediated knockdowns. Nuclear pSMAD1/5 staining was absent in *NvDpp* and *NvBMP5-8* morphants and strongly suppressed in *NvGDF5-like* morphants ([Figures 1E–1G](#)), suggesting that all three BMPs from both sides contribute to signaling via pSMAD1/5. The pSMAD1/5 staining also was abolished upon knockdown of *NvChd* ([Figure 1H](#)), suggesting that BMP signaling depends on the pro-BMP action of Chordin at a distance. Conversely, in *NvGrm* knockdowns, the pSMAD1/5-positive domain expanded in comparison to embryos injected with standard control morpholino (StdMO) ([Figures 1I–1K](#)), suggesting that Gremlin locally restricts BMP signaling. We then quantified pSMAD1/5 staining intensity in endodermal nuclei on confocal sections of control and morphant

embryos and showed a BMP signaling gradient along the directive axis, which was abolished upon injection of DppMO, suppressed in GDF5IMO and expanded in GrmMO, with significantly ($p < 0.05$, Wilcoxon exact test) elevated pSMAD1/5 levels at middle positions ([Figures 2](#) and [S2B–S2D](#)).

By late planula stage, the anlagen of the eight endodermal folds called mesenteries are formed in *Nematostella*. Phalloidin staining showed that all control late planulae contained eight mesenteries ([Figure 2A](#)), whereas no mesenteries formed in DppMO, BMP5-8MO, and ChdMO planulae ([Figures 2B](#), [S2E](#), and [S2F](#)). Strikingly, upon knockdown of *NvGDF5-like*, which leads to a much shallower gradient of pSMAD1/5, only four mesenteries were formed ([Figure 2C](#)). Knockdown of *NvGrm*, which results in an expanded pSMAD1/5 gradient, led to impaired outgrowth of mesenteries and inflated mesogloea (the normally thin extracellular matrix separating the ectodermal and endodermal layers) ([Figure 2D](#)). This demonstrates that BMP signaling is necessary for the formation and positioning of the mesenteries.

Hox Genes Are Regulated by BMP Signaling

In early planula, *NvHoxB*, *NvHoxD*, and *NvHoxE* are expressed endodermally in staggered domains along the directive axis together with *NvGbx*, demarcating the positions of future

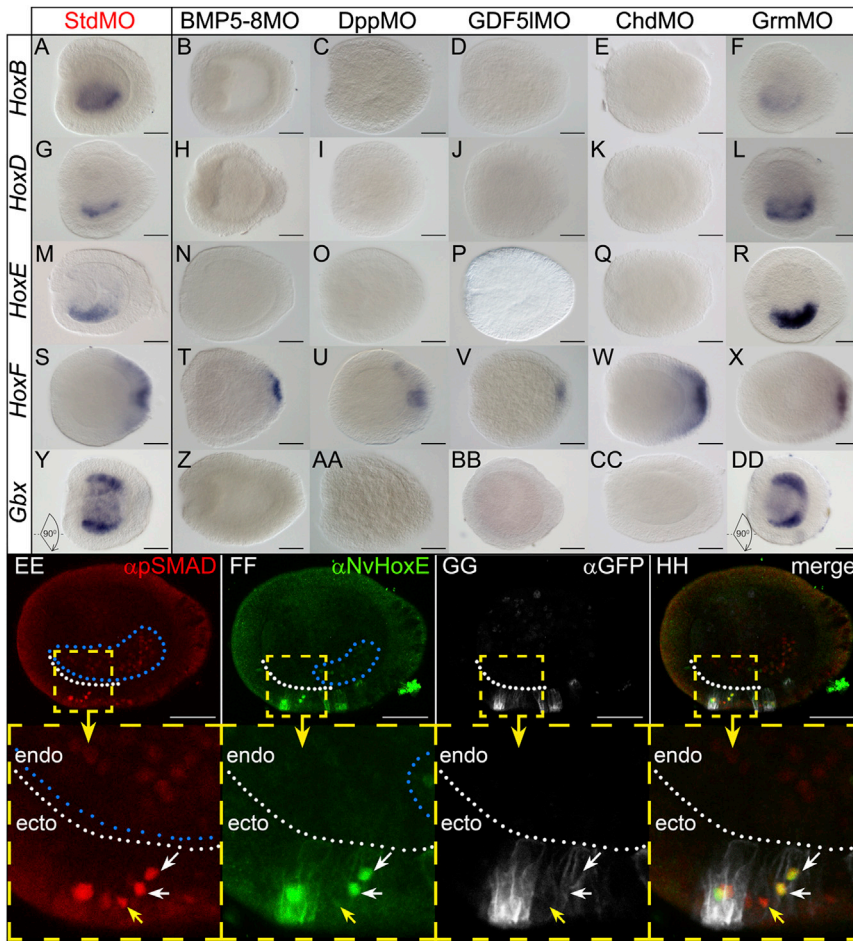


Figure 3. Staggered Endodermal Expression of *Hox* Genes and *NvGbx* Is Regulated by BMP Signaling

(A–DD) Expression of *NvHoxB* (A–F), *NvHoxD* (G–L), *NvHoxE* (M–R), *NvHoxF* (S–X), and *NvGbx* (Y–DD) in StdMO-, BMP5-8MO-, DppMO-, GDF5IMO-, ChdMO-, and GrmMO-injected embryos at early planula stage. Lateral views; oral end to the left. Embryos on (Y) and (DD) are rotated 90° compared to other stained embryos to make bilateral expression of *NvGbx* visible.

(EE–HH) Ectopic expression of BMPRI_{Q209} > D-EGFP in patches of ectodermal cells in 2-day planula results in ectopic activation of *NvHoxE* protein. (EE) Ectopic pSMAD1/5-positive nuclei in the ectoderm of early planula in addition to endogenous staining in the endoderm (blue dots). (FF) In addition to endogenous α *NvHoxE* staining (blue dots), ectopic expression is observed in pSMAD1/5-positive ectodermal nuclei. Apart from specific nuclear *NvHoxE* signal, the secondary anti-rat antibody cross-reacts with mouse anti-GFP antibody staining the BMPRI_{Q209} > D-EGFP fusion protein in the cell membranes. (GG) Anti-GFP antibody detects BMPRI_{Q209} > D-EGFP in cell membranes. Anti-mouse antibody does not cross-react with the rat α *NvHoxE*, thus no nuclear staining is observed, showing that nuclear staining on (FF) is specific for *NvHoxE*. (HH) Merged image of (EE–GG). White dots indicate the border between ectoderm and endoderm. White arrows point at two strongly pSMAD1/5-positive ectodermal nuclei in transgenic cells, which also ectopically express *NvHoxE*. Yellow arrows point at a weakly pSMAD1/5-positive ectodermal nucleus in a transgenic cell, which does not express detectable amounts of *NvHoxE*. Scale bars represent 50 μ m. See also Figure S3.

mesenteries (Ryan et al., 2007; Figures 1C and S1A; Table S2), while *NvHoxF* is expressed in a radially symmetric domain in the aboral ectoderm (Ryan et al., 2007; Figure 1C; Table S2). Whenever pSMAD1/5 staining was abolished, *NvHoxE* also could not be detected (Figures 1E–1K), suggesting that *NvHoxE* expression is downstream of BMP signaling.

To test whether other *Hox* genes also might be controlled by BMP signaling, we assessed their expression upon knockdown of BMP network members. We found that the aboral ectodermal expression of *NvHoxF* is not abolished by any of the knockdowns (Figures 3S–3X and S3). However, all endodermally, asymmetrically expressed *Hox* genes, as well as *NvGbx*, are abolished or strongly suppressed in BMP5-8MO, DppMO, GDF5IMO, and ChdMO (Figures 3A–3E, 3G–3K, 3M–3Q, 3Y–3CC, and S3). In contrast, upon knockdown of *NvGrm*, the endodermal *Hox* genes are either barely affected (*NvHoxB*, *NvHoxD*) or enhanced and broadened (*NvHoxE*) (Figures 3F, 3L, 3R, 3X, 3DD, and S3).

To test whether BMP signaling is sufficient to activate *Hox* gene expression, we overexpressed a constitutively active BMP receptor type I fused C-terminally to EGFP (BMPRI_{Q209} > D-EGFP) in a mosaic fashion in the embryo and assayed for *NvHoxE* protein. We found that, in addition to the endogenous endodermal domain, *NvHoxE* protein was detected ectopically in the nuclei

of the transgenic ectodermal cells, concurrent with the strong expression of pSMAD1/5 (Figures 3EE–3HH). Together, these data show that BMP signaling is necessary for endodermal *Hox* gene expression and sufficient to induce at least *NvHoxE*. The regulation of axial *Hox* gene expression by BMP signaling is unexpected, as so far the only known upstream regulatory role of BMP signaling on *Hox* genes is the transient and likely indirect activation of *Hox* genes in the non-organizer mesoderm in *Xenopus* (Wacker et al., 2004).

The Topology of the BMP Signaling Network

To understand the regulatory interactions required for maintaining a stable BMP signaling gradient patterning the directive axis in early planulae, we assessed expression of *NvGDF5-like*, *NvBMP5-8*, *NvDpp*, *NvChd*, and *NvGrm* upon knockdown of each of them (Figures 4A and S3).

NvDpp, *NvBMP5-8*, and *NvChd* expression (Figure 4A, images 7, 13, and 19) was restricted to the side of weak BMP signaling (Figures 1B and 1D). MO knockdown of *NvDpp* and *NvBMP5-8* resulted in upregulation and radialization of *NvDpp*, *NvBMP5-8*, and *NvChd* expression (Figure 4A, images 8–9, 14–15, and 20–21), suggesting that strong BMP signaling suppresses transcription of these genes. In contrast, *NvGDF5-like*

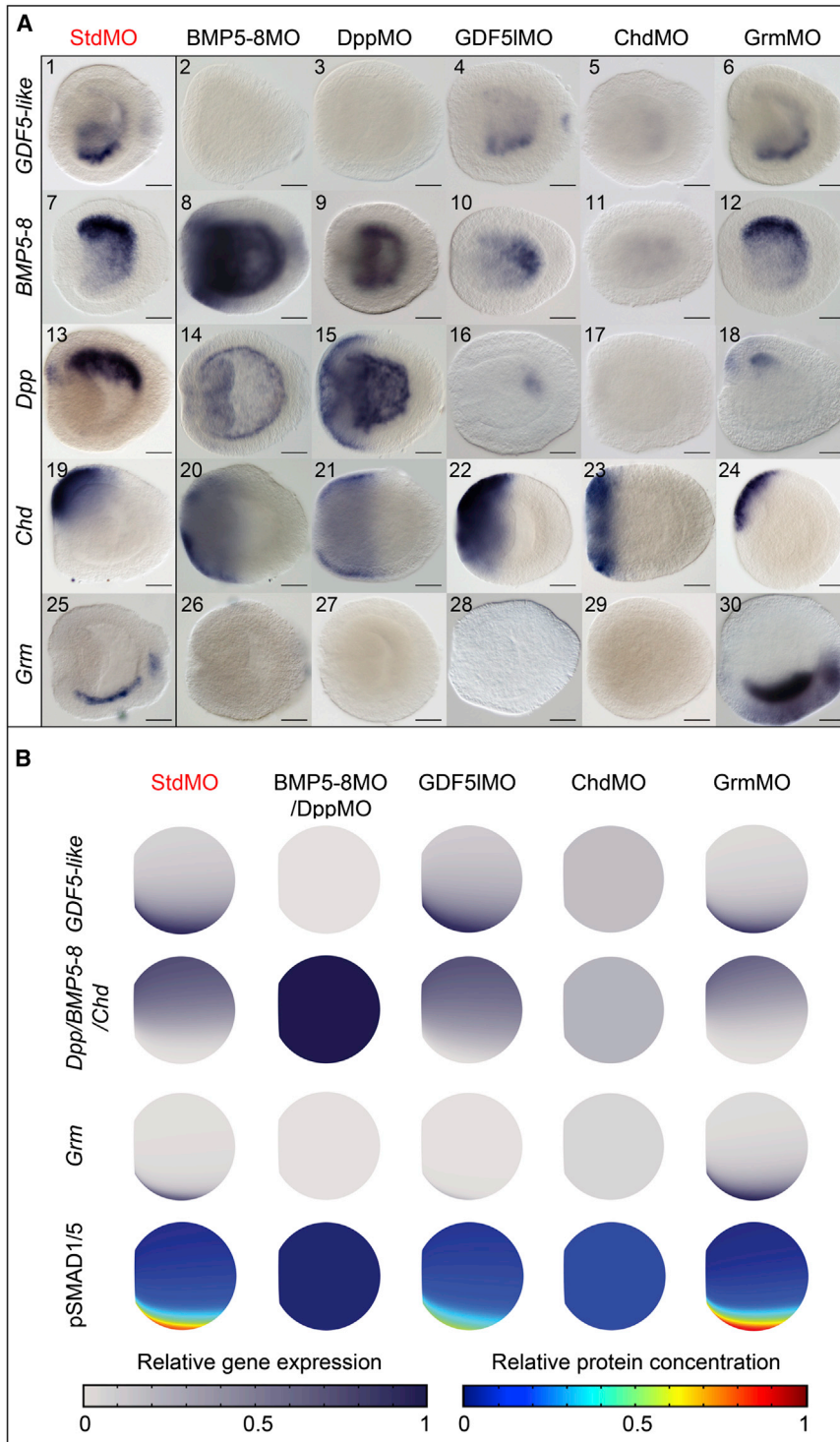


Figure 4. Maintenance of the Directive Axis in *Nematostella*

(A) Expression analysis of network components in morphant early planulae; lateral views, oral end is to the left. Scale bars represent 50 μ m.

(B) Mathematical model correctly predicts expression patterns of all genes shown in (A) (color code as in ISH), as well as pSMAD1/5 localization (shown as heat maps) in the knockdowns. All expression patterns and pSMAD1/5 staining patterns are plotted onto mesoglea and shown as 2D projections of a 3D structure. Expression domains of *NvDpp*/*NvBMP5-8*/*NvChd*, although not identical, strongly overlap when plotted onto mesoglea. In the model they are controlled by the same mathematical expression and thus plotted together. See also Figures S3 and S4.

of *NvDpp*, *NvBMP5-8*, and its own expression to an asymmetric domain on one side of the directive axis and for the signaling via *NvDpp* and *NvBMP5-8* at the opposite side of the directive axis. In *Chd*MO, *NvDpp* and *NvBMP5-8* expression was suppressed (Figure 4A, images 11 and 17) and *NvChd* expression was radialized (Figure 4A, image 23). At the same time, the *NvDpp* and *NvBMP5-8* signaling target *NvGDF5-like* on the opposite side was abolished (Figure 4A, image 5). These data suggest that Chordin locally antagonizes BMP signaling by binding *NvDpp* and *NvBMP5-8*, but facilitates their function at a distance acting as a shuttle molecule, similar to the situation in *Drosophila* (Eldar et al., 2002) and *Xenopus* (Ben-Zvi et al., 2008). Given that *NvDpp* and *NvBMP5-8* are co-expressed in *Nematostella* and their MO phenotypes are indistinguishable (Saina et al., 2009; Figure 4A), it is likely that *NvDpp* and *NvBMP5-8* heterodimerize. Disappearance of the *NvDpp* and *NvBMP5-8* expression in *Chd*MO also suggests that a low level of BMP signaling facilitated by *NvChd* might be required for the proper expression of *NvDpp* and *NvBMP5-8*.

Like *NvGDF5-like*, BMP antagonist *NvGrm* is expressed opposite to *NvDpp* (Rentzsch et al., 2006; Figure 4A, image 25), and *NvGrm* expression was absent

in *GDF5LMO*, *DppMO*, *BMP5-8MO*, and *ChdMO* (Figure 4A, images 26–29). However, *NvGDF5-like* knockdowns still showed *NvBMP5-8* and *NvDpp* expression (Figure 4A, images 10 and 16), but lacked *NvGrm* expression (Figure 4A, image 28), suggesting that in early planula *NvGrm* is induced only by

expression was restricted to the side of maximal pSMAD1/5 (Figures 1B, 1D, and 4A, image 1). *NvGDF5-like* transcription in early planula is regulated by signaling via *NvDpp* and *NvBMP5-8* as it was absent in the *BMP5-8MO* and the *DppMO* (Figure 4A, images 2–3). Chordin appeared to be pivotal for both the restriction

NvGDF5-like signaling. *NvGDF5-like* expression is not affected in GrmMO (Figure 4A, image 6), suggesting that NvGrm does not antagonize the NvDpp/NvBMP5-8 complex as otherwise NvGrm knockdown would lead to an upregulation of *NvGDF5-like*. Instead, NvGrm appears to antagonize NvGDF5-like signaling, as *NvGrm* was strongly upregulated in GrmMO (Figure 4A, image 30), suggesting enhanced NvGDF5-like signaling. NvGDF5-like signaling does not regulate *NvGDF5-like* expression as neither in GDF5LMO nor in GrmMO was *NvGDF5-like* expression affected (Figure 4A, images 4 and 6).

NvGDF5-like and *NvGrm* knockdowns indicate the contribution of NvGDF5-like to the formation of the weak BMP signaling on the *NvDpp*-expressing side of the planula. Both GDF5LMO and GrmMO resulted in a reduction of the unilateral *NvDpp*-expressing domain to the aboral or oral endoderm, respectively (Figure 4A, images 16 and 18). *NvChd* expression is suppressed by NvGDF5-like signaling, since the *NvChd* expression domain was radially expanded in GDF5IMO and not in GrmMO (Figure 4A, images 22 and 24).

Modeling Reveals Constraints of the Network

Given the complexity of the network interactions, we resorted to mathematical modeling to reveal functional constraints on the components of the BMP network. We used our loss-of-function data to generate a 3D computational model of BMP signaling-dependent maintenance of the directive axis in *Nematostella*. Our results suggest that Chordin acts as a shuttle for the Dpp/BMP5-8 heterodimer, similar to the situation in *Drosophila* and *Xenopus* during DV patterning (Ben-Zvi et al., 2008; Eldar et al., 2002; Iber and Gaglia, 2007; Mizutani et al., 2005). A mathematical model for BMP ligand shuttling by Mizutani and co-workers focuses on the core part of the regulatory network and reproduces the kinetics of the maintenance of the BMP signaling in *Drosophila* correctly (Iber and Gaglia, 2007; Mizutani et al., 2005). To test whether similar rules also would apply to a non-bilaterian, we adapted the model to *Nematostella* (Figure S4A, black part) by including NvGDF5-like and NvGrm (Figure S4A, colored part) in addition to NvDpp, NvBMP5-8, and NvChd and by removing Twisted gastrulation (Tsg), as Tsg is absent from the *Nematostella* genome (Putnam et al., 2007). Our aim was to include these components with the least alterations to the *Drosophila* model in a way that all key experimental observations in control and MO experiments in *Nematostella* could be reproduced and thus generate a minimal viable model of BMP signaling maintenance in *Nematostella* after symmetry break (see the Supplemental Experimental Procedures for details).

According to the core model (Figure S4A, black part), the diffusible NvDpp/NvBMP5-8 heterodimer (termed BMP in the schemes) can either form an inactive diffusible complex with NvChd, or bind the BMP receptor to form an active signaling complex and undergo degradation (for details see the Supplemental Experimental Procedures). As in other systems, NvChd, when bound to the NvDpp/NvBMP5-8 ligand, is cleaved by ubiquitously endodermally expressed Tollid (Matus et al., 2006b) to release the active BMP heterodimer. After the simulation start, shuttling of NvDpp/NvBMP5-8 by Chordin rapidly results in a stable BMP signaling gradient with a maximum opposite to the *NvChd* expression domain (Figure S4), consistent with the

experimentally observed pSMAD1/5 distribution. BMP signaling then represses *NvChd* expression (Figure S4A, red dashed lines), maintaining the restricted expression patterns. The initial restriction on *NvChd* expression needs to be imposed for only 15 min in the model. Thereafter, the simulation reproduces all important aspects of the expression of *NvDpp*, *NvBMP5-8*, *NvGDF5-like*, *NvChd*, and *NvGrm*, as well as the location of the BMP signaling domain in the wild-type and the knockdowns (Figures 4B and S4), confirming the role of each of the BMPs and the BMP antagonists in maintaining and shaping the pSMAD1/5 gradient. Thus, we conclude that the deduced topology of the *Nematostella* BMP network (Figure 5A) is consistent with the experimental data.

To assess the sensitivity of the signaling network to perturbation, we systematically increased and decreased all 31 model parameters individually until the model failed to reproduce asymmetric BMP signaling (Figures 5F and S5A). In line with the results of the knockdowns (Figures 3A–3F), many of the parameters linked to NvDpp/NvBMP5-8 and NvChd were heavily constrained, while those related to NvGDF5-like and NvGrm could vary widely without destroying the asymmetric BMP signaling pattern (Figures 5F and S5A).

To test whether a division into constrained core components and unconstrained modulators might represent a conserved evolutionary feature of axis-forming BMP signaling networks, we adapted the model to describe the BMP network regulating DV patterning in frog embryos. As for *Nematostella*, our minimal viable model describing the *Xenopus* BMP network using a subset of the components (for details see the Supplemental Experimental Procedures) reproduced all key aspects of normal expression as well as known loss-of-function and overexpression phenotypes of BMP4/BMP7, ADMP/BMP2, Chordin, SMAD6/7, and BAMBI (Khokha et al., 2005; Paulsen et al., 2011; Reversade and De Robertis, 2005; Figures S4B and S4J). The sensitivity analysis demonstrated that in frog, like in *Nematostella*, there is a conserved core of the network with strongly constrained parameters (BMPs, Chordin, Tollid) and peripheral weakly constrained signaling modulators, such as BAMBI and SMAD6/7 (Figures 5F, 5G, and S5).

DISCUSSION

Similar to Bilateria, anthozoans have a second body axis specified by BMP signaling (Saina et al., 2009; Leclère and Rentzsch, 2014). We have shown that various BMPs and BMP antagonists from opposing sides of the *Nematostella* larva contribute to the maintenance of nuclear pSMAD1/5 gradient along the directive axis. This could be interpreted as evidence for common evolutionary origin of the directive and DV axis and loss of bilaterality in medusozoan cnidarians, such as hydroids and jellyfish. The deduced topology of the BMP network maintaining the directive axis in *Nematostella* appears to be remarkably similar to the one described for the DV-patterning network in *Xenopus* (Reversade and De Robertis, 2005; Zakin and De Robertis, 2010; Figures 5A and 5B). However, striking differences in the BMP networks exist between Bilateria and Cnidaria: (1) conserved molecules occupy different positions in the network and there is a positive-versus-negative feedback loop of BMP4/BMP5-8 on their

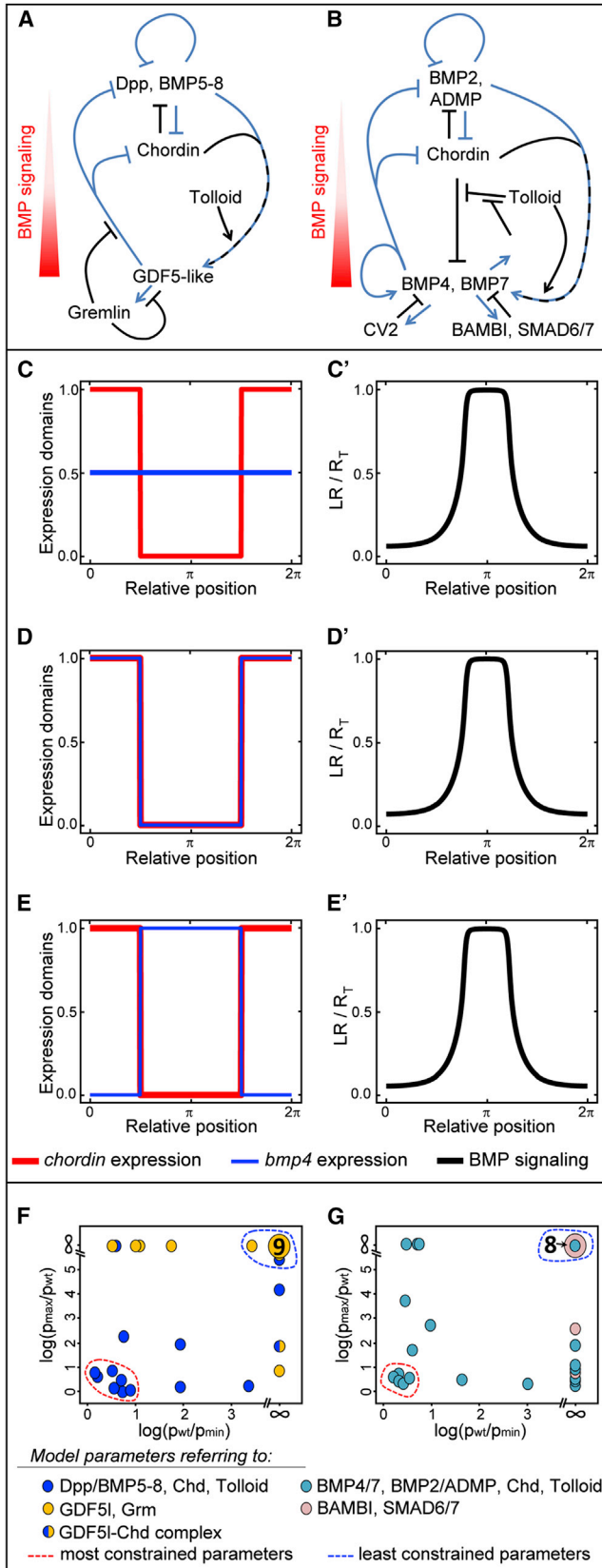


Figure 5. Strongly Constrained Core Interactions and Weakly Constrained Modulators of the BMP Signaling System

(A and B) *Nematostella* directive axis network (A) compared to the DV network in *Xenopus* (B). Blue lines represent transcriptional regulation downstream of BMP signaling and black lines represent protein-protein interactions (putative in case of *Nematostella*). *Xenopus* network is modified after (De Robertis and Colozza, 2013; Paulsen et al., 2011). Overlaid blue and black lines represent shuttle function of Chordin.

(C–E) Restricted *chordin* expression domain (red curves on the left plots) results in BMP signaling on the opposite side of the embryo (relative concentration of BMP ligand-receptor complexes shown as black curves on C'–E') independent of *bmp4* expression localization (blue curve). *bmp4* can be expressed uniformly (C), on the *chordin* side (D), or opposite to it (E). The x axis is normalized with respect to maximal domain length (shown as 2π since the embryo is spherical), and the y axis shows the ratio of ligand-bound receptors (LR) with respect to total receptor concentration (R_T).

(F and G) Constrained core regulators versus weakly constrained modulators of BMP signaling in *Nematostella* (F) and *Xenopus* (G).

(F) Many parameters describing production, function, and turnover of NvDpp/NvBMP5-8 and NvChd (blue circles) are strongly constrained, while most of the parameters describing production, function, and turnover of NvGDF5-like and NvGrm (orange circles) are weakly constrained. Large orange circle with a 9 corresponds to nine unconstrained parameters related to NvGDF5-like and NvGrm.

(G) Many parameters describing production, function, and turnover of frog BMP4/BMP7, ADMP/BMP2, Chordin, and Tolloid (teal circles) are strongly constrained, while most of the parameters describing production, function, and turnover of BAMBI and SMAD6/7 (pink circles) are weakly constrained. Large pink circle with an 8 corresponds to eight unconstrained parameters related to BAMBI and SMAD6/7. Fold of possible increase of parameter values (log scale) is plotted on the y axis, and fold of possible decrease of parameter values (log scale) is plotted on the x axis. (For details see the Supplemental Experimental Procedures and Figure S5.)

See also Figure S5.

own expression; (2) the involvement of Gdf5 and Gremlin homologs in the initial axis specification, although not unique, is very uncommon in Bilateria (Kuo and Weisblat, 2011; Sidi et al., 2003); and (3) instead of positioning the CNS, in *Nematostella*, the gradient of BMP signaling is used to specify and position the mesenteries and regulate staggered Hox and Gbx gene expression in the endoderm. This link of an early BMP gradient and staggered Hox gene expression is uncommon among Bilateria, where Hox genes are a hallmark of patterning the anterior-posterior axis, but not the DV axis. All these differences make homology assumptions of the cnidarian and bilaterian axes problematic.

Combination of gene function analysis and mathematical modeling allows insights into how BMP signaling networks evolved in different animals. One of the obvious differences in the organization of the BMP signaling systems during secondary body-axis patterning in different organisms is the relative location of the *bmp4* and *chordin* expression domains. While in Bilateria *bmp4* and *chordin* are typically expressed on opposing ends of the DV axis (De Robertis, 2008), they are co-expressed in *Nematostella* (Rentzsch et al., 2006) and sea urchin (Lapraz et al., 2009), raising questions about the ancestral mode of *bmp4* and *chordin* expression in Bilateria (Figure 1A). Our 1D computational analysis of differently positioned *bmp4* and *chordin* expression domains reveals, however, that only the spatial restriction of *chordin* expression is crucial, while the

BMP expression domain can vary; BMP signaling maximum always is located opposite to the *chordin* expression domain independent of the *bmp4* expression pattern if shuttling is at work (Figures 5C–5E). This suggests that there is no selection pressure on the localization of *bmp4*, as long as *chordin* expression is restricted. Support for this conclusion comes from experiments in *Drosophila* showing that the BMP signaling domain is defined solely by *Sog* expression (Wang and Ferguson, 2005), and in *Nematostella* demonstrating that ChdMO injected into one half of the embryo always leads to the formation of the pSMAD1/5-positive domain on the injection side; i.e., where Chordin protein is inactive (Leclère and Rentzsch, 2014).

Sensitivity analysis of our model demonstrated that, consistent with the knockdown phenotypes, the parameters describing production and turnover of NvDpp/NvBMP5-8 and NvChd, which are required for generating the BMP signaling gradient, were strongly constrained (Figures 5F and S5A), while those describing NvGDF5-like and NvGrm, which work as modulators of the BMP signaling, could vary widely (Figures 5F and S5A). Modeling frog BMP signaling network, based on the same principles of ligand shuttling, showed that the same logic of having highly constrained core components and weakly constrained modulators of the BMP signaling also applied here and thus might be a common theme throughout animal evolution (Figures 5G and S5B). An important difference between the *Xenopus* and *Nematostella* networks is that the frog system appears to be more robust due to partial redundancy of the BMP ligands. Different constraints on members of the BMP network give clues as to why BMP signaling modulators seem to be exchanged easily during evolution in various animals, while the involvement of the core components, BMP4 and Chordin, is conserved except for a few known cases, primarily in animals with highly deterministic development like leeches, ascidians, and nematodes (Kuo and Weisblat, 2011; Lemaire, 2009; Patterson and Padgett, 2000), but also in the wasp *Nasonia* (Özük et al., 2014). In this respect, investigating the DV-patterning mechanism in molluscs, which develop similar to annelids but, unlike annelids, have retained *chordin* in their genomes, will be particularly interesting.

In summary, we deciphered the logic of the BMP signaling network maintaining the secondary body axis in a non-bilaterian species, the sea anemone *Nematostella vectensis*, and demonstrated an unexpected link between BMP signaling and staggered Hox gene expression. Mathematical modeling showed that the spatial restriction of *chordin* expression as well as the production and turnover of the core components of the network appear to be the factors crucial for the functional BMP signaling system in many of the studied Eumetazoa. Since the selection pressure is on the generation of robust signaling gradients, the variety of different network topologies primarily is constrained by the biochemical qualities of the core network components. We conclude that a few key constraints under strong selection pressure keep crucial parameters constant over hundreds of millions of years of separation, while less constrained modulators are added or removed during the evolution of the BMP signaling network, thus generating the diversity of different BMP signaling networks observed in animals.

EXPERIMENTAL PROCEDURES

Animal Culture and Microinjection

Animals were kept and gametogenesis was induced as described (Genikhovich and Technau, 2009a). Antisense MO oligonucleotides (Gene Tools) against *NvDpp*, *NvBMP5-8*, *NvGDF5-like*, *NvChd*, and *NvGrm* were injected into fertilized eggs. For MO sequences, concentrations, and specificity tests as well as for the details on generating the constitutively active *Nematostella* BMPRI, see the Supplemental Experimental Procedures.

Antibody Staining, Phalloidin Staining, and In Situ Hybridization

Rabbit anti-Phospho-Smad1 (Ser463/465)/Smad5 (Ser463/465)/Smad8 (Ser426/428) (Cell Signaling, 9511), rat anti-NvHoxE, rabbit anti-GFP (Abcam, ab290), and mouse anti-GFP (Life Technologies, A11120) were used for the experiments. Intensity of α pSMAD1/5 staining was quantified on 16-bit images of confocal optical sections (oral views) of early morphant and control planulae stained with DAPI and α pSMAD1/5. For F-actin staining, Alexa Fluor 488 phalloidin (Life Technologies, A12379) was used. For the details on raising the anti-NvHoxE antibody, the antibody staining protocol, and pSMAD1/5 gradient quantification, see the Supplemental Experimental Procedures. In situ hybridization was performed as described previously (Genikhovich and Technau, 2009b). For double in situ, the staining was developed as in Denker et al., 2008.

Mathematical Modeling

Details on the mathematical modeling are presented in the Supplemental Experimental Procedures.

ACCESSION NUMBERS

The NvBMPRI sequence has been deposited to the GenBank and is available under accession number KJ948110.

SUPPLEMENTAL INFORMATION

Supplemental Information includes Supplemental Experimental Procedures, five figures, and two tables and can be found with this article online at <http://dx.doi.org/10.1016/j.celrep.2015.02.035>.

AUTHOR CONTRIBUTIONS

G.G. and U.T. designed experiments. G.G., M.M.P., J.B.S., and A.F.G. performed experiments. G.G. analyzed data. P.F., K.M., and D.I. did mathematical modelling. D.F. performed statistical analysis of gradient data. G.G., U.T., D.I., and P.F. wrote the paper.

ACKNOWLEDGMENTS

We thank the Core Imaging Facility of the Faculty of Life Sciences; Stefanie Wienkoop for performing tandem mass spectrometry (MS/MS) of NvHoxE; Simon Weinberger for working on the antibody staining protocol; Yehu Moran, Eduard Renfer, Andy Aman, and Lucas Leclère for technical advice; Eduard Renfer and Sandra Laufer for isolating β -actin promoter; Patrick Steinmetz, Yehu Moran, and Andy Aman for critically reading the manuscript; and Fabian Rentzsch for sharing unpublished data. This work was funded by grants of the Austrian Science Foundation FWF P22717 (to U.T.) and P26962 (to G.G.) and the EU-ITN EVONET (215781) to U.T.

Received: June 23, 2014

Revised: December 17, 2014

Accepted: February 13, 2015

Published: March 12, 2015

REFERENCES

Arendt, D., and Nübler-Jung, K. (1994). Inversion of dorsoventral axis? *Nature* 371, 26.

- Ben-Zvi, D., Shilo, B.Z., Fainsod, A., and Barkai, N. (2008). Scaling of the BMP activation gradient in *Xenopus* embryos. *Nature* *453*, 1205–1211.
- De Robertis, E.M. (2008). Evo-devo: variations on ancestral themes. *Cell* *132*, 185–195.
- De Robertis, E.M., and Colozza, G. (2013). Development: scaling to size by protease inhibition. *Curr. Biol.* *23*, R652–R654.
- Denker, E., Manuel, M., Leclère, L., Le Guyader, H., and Rabet, N. (2008). Ordered progression of nematogenesis from stem cells through differentiation stages in the tentacle bulb of *Clytia hemisphaerica* (Hydrozoa, Cnidaria). *Dev. Biol.* *315*, 99–113.
- Eldar, A., Dorfman, R., Weiss, D., Ashe, H., Shilo, B.Z., and Barkai, N. (2002). Robustness of the BMP morphogen gradient in *Drosophila* embryonic patterning. *Nature* *419*, 304–308.
- Finnerty, J.R., Pang, K., Burton, P., Paulson, D., and Martindale, M.Q. (2004). Origins of bilateral symmetry: Hox and dpp expression in a sea anemone. *Science* *304*, 1335–1337.
- Genikhovich, G., and Technau, U. (2009a). In situ hybridization of starlet sea anemone (*Nematostella vectensis*) embryos, larvae, and polyps. *Cold Spring Harb Protoc* *2009*, t5282.
- Genikhovich, G., and Technau, U. (2009b). Induction of spawning in the starlet sea anemone *Nematostella vectensis*, in vitro fertilization of gametes, and jellying of zygotes. *Cold Spring Harb Protoc* *2009*, t5281.
- Hejnal, A., Obst, M., Stamatakis, A., Ott, M., Rouse, G.W., Edgecombe, G.D., Martinez, P., Baguña, J., Bailly, X., Jondelius, U., et al. (2009). Assessing the root of bilaterian animals with scalable phylogenomic methods. *Proc. Biol. Sci.* *276*, 4261–4270.
- Iber, D., and Gaglia, G. (2007). The mechanism of sudden stripe formation during dorso-ventral patterning in *Drosophila*. *J. Math. Biol.* *54*, 179–198.
- Inomata, H., Haraguchi, T., and Sasai, Y. (2008). Robust stability of the embryonic axial pattern requires a secreted scaffold for chordin degradation. *Cell* *134*, 854–865.
- Inomata, H., Shibata, T., Haraguchi, T., and Sasai, Y. (2013). Scaling of dorsal-ventral patterning by embryo size-dependent degradation of Spemann's organizer signals. *Cell* *153*, 1296–1311.
- Jazwińska, A., Kirov, N., Wieschaus, E., Roth, S., and Rushlow, C. (1999). The *Drosophila* gene *brinker* reveals a novel mechanism of Dpp target gene regulation. *Cell* *96*, 563–573.
- Khokha, M.K., Yeh, J., Grammer, T.C., and Harland, R.M. (2005). Depletion of three BMP antagonists from Spemann's organizer leads to a catastrophic loss of dorsal structures. *Dev. Cell* *8*, 401–411.
- Kuo, D.H., and Weisblat, D.A. (2011). A new molecular logic for BMP-mediated dorsoventral patterning in the leech *Helobdella*. *Curr. Biol.* *21*, 1282–1288.
- Lapraz, F., Besnardeau, L., and Lepage, T. (2009). Patterning of the dorsal-ventral axis in echinoderms: insights into the evolution of the BMP-chordin signaling network. *PLoS Biol.* *7*, e1000248.
- Leclère, L., and Rentzsch, F. (2014). RGM regulates BMP-mediated secondary axis formation in the sea anemone *Nematostella vectensis*. *Cell Rep.* *9*, 1921–1930.
- Lee, H.X., Ambrosio, A.L., Reversade, B., and De Robertis, E.M. (2006). Embryonic dorsal-ventral signaling: secreted frizzled-related proteins as inhibitors of tolloid proteinases. *Cell* *124*, 147–159.
- Lemaire, P. (2009). Unfolding a chordate developmental program, one cell at a time: invariant cell lineages, short-range inductions and evolutionary plasticity in ascidians. *Dev. Biol.* *332*, 48–60.
- Matus, D.Q., Pang, K., Marlow, H., Dunn, C.W., Thomsen, G.H., and Martindale, M.Q. (2006a). Molecular evidence for deep evolutionary roots of bilaterality in animal development. *Proc. Natl. Acad. Sci. USA* *103*, 11195–11200.
- Matus, D.Q., Thomsen, G.H., and Martindale, M.Q. (2006b). Dorso/ventral genes are asymmetrically expressed and involved in germ-layer demarcation during cnidarian gastrulation. *Curr. Biol.* *16*, 499–505.
- Mizutani, C.M., Nie, Q., Wan, F.Y., Zhang, Y.T., Vilmos, P., Sousa-Neves, R., Bier, E., Marsh, J.L., and Lander, A.D. (2005). Formation of the BMP activity gradient in the *Drosophila* embryo. *Dev. Cell* *8*, 915–924.
- Özüak, O., Buchta, T., Roth, S., and Lynch, J.A. (2014). Ancient and diverged TGF- β signaling components in *Nasonia vitripennis*. *Dev. Genes Evol.* *224*, 223–233.
- Patterson, G.I., and Padgett, R.W. (2000). TGF beta-related pathways. Roles in *Caenorhabditis elegans* development. *Trends Genet.* *16*, 27–33.
- Paulsen, M., Legewie, S., Eils, R., Karaulanov, E., and Niehrs, C. (2011). Negative feedback in the bone morphogenetic protein 4 (BMP4) synexpression group governs its dynamic signaling range and canalizes development. *Proc. Natl. Acad. Sci. USA* *108*, 10202–10207.
- Philippe, H., Brinkmann, H., Copley, R.R., Moroz, L.L., Nakano, H., Poustka, A.J., Wallberg, A., Peterson, K.J., and Telford, M.J. (2011). Acoelomorph flatworms are deuterostomes related to *Xenoturbella*. *Nature* *470*, 255–258.
- Piccolo, S., Sasai, Y., Lu, B., and De Robertis, E.M. (1996). Dorsoventral patterning in *Xenopus*: inhibition of ventral signals by direct binding of chordin to BMP-4. *Cell* *86*, 589–598.
- Piccolo, S., Agius, E., Lu, B., Goodman, S., Dale, L., and De Robertis, E.M. (1997). Cleavage of Chordin by Xolloid metalloprotease suggests a role for proteolytic processing in the regulation of Spemann organizer activity. *Cell* *91*, 407–416.
- Plouhinec, J.L., Zakin, L., and De Robertis, E.M. (2011). Systems control of BMP morphogen flow in vertebrate embryos. *Curr. Opin. Genet. Dev.* *21*, 696–703.
- Putnam, N.H., Srivastava, M., Hellsten, U., Dirks, B., Chapman, J., Salamov, A., Terry, A., Shapiro, H., Lindquist, E., Kapitonov, V.V., et al. (2007). Sea anemone genome reveals ancestral eumetazoan gene repertoire and genomic organization. *Science* *317*, 86–94.
- Rentzsch, F., Anton, R., Saina, M., Hammerschmidt, M., Holstein, T.W., and Technau, U. (2006). Asymmetric expression of the BMP antagonists chordin and gremlin in the sea anemone *Nematostella vectensis*: implications for the evolution of axial patterning. *Dev. Biol.* *296*, 375–387.
- Reversade, B., and De Robertis, E.M. (2005). Regulation of ADMP and BMP2/4/7 at opposite embryonic poles generates a self-regulating morphogenetic field. *Cell* *123*, 1147–1160.
- Ryan, J.F., Mazza, M.E., Pang, K., Matus, D.Q., Baxeavanis, A.D., Martindale, M.Q., and Finnerty, J.R. (2007). Pre-bilaterian origins of the Hox cluster and the Hox code: evidence from the sea anemone, *Nematostella vectensis*. *PLoS ONE* *2*, e153.
- Saina, M., Genikhovich, G., Renfer, E., and Technau, U. (2009). BMPs and chordin regulate patterning of the directive axis in a sea anemone. *Proc. Natl. Acad. Sci. USA* *106*, 18592–18597.
- Sidi, S., Goutel, C., Peyriéras, N., and Rosa, F.M. (2003). Maternal induction of ventral fate by zebrafish radar. *Proc. Natl. Acad. Sci. USA* *100*, 3315–3320.
- Wacker, S.A., McNulty, C.L., and Durston, A.J. (2004). The initiation of Hox gene expression in *Xenopus laevis* is controlled by Brachyury and BMP-4. *Dev. Biol.* *266*, 123–137.
- Wang, Y.C., and Ferguson, E.L. (2005). Spatial bistability of Dpp-receptor interactions during *Drosophila* dorsal-ventral patterning. *Nature* *434*, 229–234.
- Zakin, L., and De Robertis, E.M. (2010). Extracellular regulation of BMP signaling. *Curr. Biol.* *20*, R89–R92.